HHS Public Access

Author manuscript

Eur J Neurosci. Author manuscript; available in PMC 2019 August 12.

Published in final edited form as:

Eur J Neurosci. 2018 March ; 47(5): 427–432. doi:10.1111/ejn.13848.

Early Blindness is Associated with Increased Volume of the Uncinate Fasciculus

Corinna M. Bauer[1], **Zaira Cattaneo**[2,3], **Lotfi B. Merabet**[1]

[1]Laboratory for Visual Neuroplasticity. Department of Ophthalmology, Massachusetts Eye and Ear Infirmary, Harvard Medical School, Boston, MA, USA

[2]Department of Psychology, University of Milano-Biococca, Milan 20126, Italy.

[3]Brain Connectivity Center, C. Mondino National Neurological Institute, Pavia 27100, Italy.

Abstract

Growing evidence demonstrates dramatic structural and functional neuroplastic changes in individuals born with early onset blindness. For example, crossmodal sensory processing at the level of the occipital cortex appears to be associated with adaptive behaviors in the blind. However, detailed studies examining the structural properties of key white matter pathways in other regions of the brain remain limited. Given that blind individuals rely heavily on their sense of hearing, we examined the structural properties of two important pathways involved with auditory processing namely, the uncinate and arcuate fasciculi. High angular resolution diffusion imaging (HARDI) tractography was used to examine structural parameters (i.e. tract volume and quantitative anisotropy, or QA) of these two fasciculi in a sample of 13 early blind individuals and 14 normally sighted controls. Compared to controls, early blind individuals showed a significant increase in the volume of the left uncinate fasciculus. A small area of increased QA was also observed half way along the right arcuate fasciculus in the blind group. These findings contribute to our knowledge regarding the broad neuroplastic changes associated with profound early blindness.

Keywords

uncinate fasciculus; arcuate fasciculus; early blindness; HARDI tractography

Introduction

Growing evidence suggests that the brain undergoes dramatic structural and functional changes as a result of profound early blindness. For example, studies using diffusion

Corresponding Author: Corinna M. Bauer, 20 Staniford Street, Boston, MA 02114, 617-573-4072 (phone), 617-912-0111 (facsimile), Corinna_Bauer@meei.harvard.edu.

Author Contributions

All authors contributed to the study design, analysis, and preparation of the manuscript.

Conflict of Interest Statement

The authors have no financial conflicts of interest to declare.

Data Accessibility Statement

Data and materials will be made available if in accordance with the Internal Review Board of Massachusetts Eye and Ear Infirmary.

tractography have reported evidence of increased white matter connectivity between the occipital cortex and other areas of the brain such as frontal cortical regions (Ptito *et al.*, 2008; Bauer *et al.*, 2017). Similarly, tracer studies in visually deprived animal models (e.g. neonatally binocularly enucleated opossums) have demonstrated the existence of increased direct inputs from auditory, somatosensory, and multimodal cortical areas with the occipital cortex (Karlen *et al.*, 2006). Functionally, numerous studies have shown that the occipital cortex is recruited for the processing of non-visual sensory information, as well as for cognitive tasks including memory and language (e.g. 2010; Ricciardi *et al.*, 2014; Bauer *et al.*, 2015; for review see Merabet & Pascual-Leone). Together, these studies highlight the role of the occipital cortex in crossmodal sensory processing and may represent an important neurophysiological substrate related to the adaptive behaviors observed in individuals who are blind (Voss & Zatorre, 2012). However, studies examining the structural properties of key white matter pathways implicating other sensory modalities and regions of the brain remain limited. For example, blind individuals are highly reliant on their sense of hearing as a means to acquire information about their surroundings. Thus, one may expect to observe differences in the structural properties of white matter pathways implicated in auditory processing.

The auditory system is associated with two prominent white matter pathways namely, the arcuate and uncinate fasciculi. Both these pathways connect frontal to temporal cortices, but support different functions. The arcuate fasciculus constitutes the neuroanatomical correlate of the dorsal auditory pathway (Hickok & Poeppel, 2004) and is implicated in complex syntactic processes (Wilson *et al.*, 2011), auditory-to-motor mapping (Geschwind, 1965), speech fluency (Fridriksson *et al.*, 2013), and speech production (Marchina *et al.*, 2011). Fibers of the arcuate fasciculus curve around the Sylvian fissure, connecting Wernicke's area with Broca's area (Fernández-Miranda *et al.*, 2015). In contrast, the uncinate fasciculus is believed to represent the neuroanatomical correlate of the ventral auditory stream (Hickok & Poeppel, 2004), arching around the insula and connecting the frontal lobe to the anterior temporal lobe (Hau *et al.*, 2016). Establishing the specific role of the uncinate fasciculus remains a topic of debate (Von Der Heide *et al.*, 2013) and this pathway is likely involved with a number of functions, such as auditory and verbal working memory (Schaeffer *et al.*, 2014) and semantic processing, including naming of objects and people (Papagno, 2011). Evidence also suggests that the uncinate fasciculus may be involved with reading, sound recognition, spatial navigation, and social and affective processes (see (Von Der Heide *et al.*, 2013; Olson *et al.*, 2015) for reviews).

In this study, we employed high angular resolution diffusion imaging (HARDI) (Tuch *et al.*, 2002) and white matter fiber reconstruction methodologies to characterize properties related to the structural integrity (i.e. tract volume and average quantitative anisotropy; or QA) of the arcuate and uncinate fasciculi in early blind individuals compared to normally sighted controls. While both HARDI and diffusion tensor imaging (DTI) techniques provide information regarding the degree of water diffusivity in the brain in order to derive local axonal fiber orientation, HARDI utilizes a stronger diffusion gradient than DTI and is able to resolve multiple fiber orientations within each voxel (Tuch *et al.*, 2002). Thus, it has become increasingly established that HARDI is superior to DTI in its ability to delineate crossing

fibers and ultimately the overall microarchitecture of the brain (Tuch *et al.*, 2002; Berman *et al.*, 2013; Seunarine & Alexander, 2014).

While this is an exploratory analysis, we hypothesize that there will be significant differences in white matter integrity of auditory pathways in early blind individuals compared to normally sighted controls

Materials and Methods

Study participants

Thirteen early blind (6 females, mean age: 33.62 years, age range: 25–46 years) and 14 normally sighted controls (6 females, mean age: 29.21 years, age range: 19–44 years) took part in the experiment. The blind and sighted control groups did not significantly differ in terms of age ($t(25) = -1.54$, $p = 0.14$) or gender (Chi-square = 0.03, $p = 0.86$). While the majority of the blind participants had diagnoses that could be considered of "congenital" cause, for the purposes of this study "early blindness" was defined as clinically documented residual visual functioning no greater than light perception and/or hand motion perception acquired prior to the age of three. The etiologies of blindness were varied and included retinal dystrophies as well as ocular malformations (see Table 1). Apart from blindness, the participants had no documented cognitive or neurological abnormalities. Sighted controls had normal or corrected-to-normal visual acuity.

Written informed consent was obtained from all subjects prior to participation, and all experimental procedures were approved by the Institutional Review Board at the Massachusetts Eye and Ear Infirmary, Boston, MA, USA, and conformed with the World Medical Association Declaration of Helsinki.

MRI acquisition and analysis

All imaging data were acquired on a 3T Philips Achieva System (Best, the Netherlands) with an 8-channel phased array coil. Two structural T_1-weighted scans were acquired using a turbo spin echo sequence (TE = 3.1 ms, TR = 6.8 ms, flip angle = 9°, voxel size 0.98 × 0.98 × 1.20 mm) and HARDI was acquired with a single-shot EPI sequence (TE = 73 ms, TR = 17,844 ms, flip angle 90°, 64 directions, EPI factor = 59, Bmin = 0 s/mm2, Bmax = 3,000 s/mm2, voxel size = 2 mm isotropic, enhanced gradients at 80 mT/m, and a slew rate of 100 T/m/ms).

HARDI data were skull-stripped and corrected for eddy currents in FSL 5.0.8 (FMRIB Software Library, http://fsl.fMRib.ox.ac.uk/fsl). Motion was less than a voxel (i.e. 2 mm) for each subject and contained no large spikes (absolute motion = 1.14 mm ± 0.27 SD, relative motion = 0.69 ± 0.21 SD. The orientation distribution function (ODF) was reconstructed in DSI-Studio (http://dsi-studio.labsolver.org) using generalized q-sampling imaging (Yeh *et al.*, 2010) with a diffusion sampling length ratio of 1.25, ODF sharpening via decomposition (Yeh & Tseng, 2013), decomposition fraction of 0.04, and maximum fiber population of 8. Three fibers per voxel were resolved with an 8-fold ODF tessellation. HARDI data were co-registered to the corresponding T_1-weighted structural image for each subject using boundary-based registration in FreeSurfer (Greve & Fischl, 2009). Registration accuracy

was verified for each subject and manual corrections were performed where necessary. Each of the 68 cortical T_1-weighted parcellations (Desikan *et al.*, 2006) were reverse transformed into subject-specific HARDI space, creating the seed (start) and target (end) point regions of interests (ROIs) for tractography analysis.

An in-house MATLAB script utilizing the tractography function from DSI-Studio generated streamlines between the ROIs (see below) with the following user-defined parameters: termination angle of 45°, subject-specific QA threshold (Abhinav *et al.*, 2014), smoothing of 0.5, step size 0.5 mm, minimum length = 5 mm, maximum length = 300 mm, random fiber direction, Gaussian radial interpolation, and 100,000 seeds. Tract volume and mean QA were examined for each reconstructed fasciculus bilaterally based on calculations in DSI-Studio, whereby tract volume is calculated based on the number of voxels containing a fiber (Volume = N_{voxels} × voxel size) and mean QA is the average of QA values samples at tract coordinates.

Parcellation of fasciculi

The arcuate fasciculus was defined using start seeds of the pars opercularis, pars triangularis, medial orbitofrontal, caudal middle frontal, and precentral gyrus with target seeds of the supramarginal gyrus, banks of the superior temporal sulcus, transverse temporal, as well as the inferior, middle, and superior temporal gyri (Kamali *et al.*, 2014; Fernández-Miranda *et al.*, 2015).

The uncinate fasciculus was defined using start seeds of the lateral orbitofrontal, medial orbitofrontal, pars opercularis, pars triangularis, pars orbitalis, rostral middle frontal, and frontal pole with target seeds of the entorhinal cortex, fusiform, inferior temporal, superior temporal, temporal pole, and transverse temporal (Hau *et al.*, 2016).

All tractography seeds were generated from the Desikan atlas (Desikan *et al.*, 2006). Reconstructed fibers for each subject were visually assessed for accuracy. Any fibers not belonging to the fasciculi of interest (e.g. from the extreme capsule) were removed.

Statistical Analysis

Statistical analyses were performed in SAS University Edition running on an Oracle VM VirtualBox. In order to remove the potential effects of head size, residuals of total intracranial volume (as calculated in FreeSurfer) were computed for tract volume (Sanfilipo *et al.*, 2004; Pintzka *et al.*, 2015). Note that the means of the residuals average to zero, resulting in negative and positive values. Equality of variances was assessed with a folded F-test. If variances were equal, a two-sample pooled t-test was used, while a Satterthwaite t-test was used in instances of unequal variance. Bonferroni correction was used for multiple comparisons, and results were considered significant at a threshold of $p < 0.05$. Finally, a series of t-tests were used to examine the possible effect of hemispheric laterality within each group on tract volume and mean QA measures of the arcuate and uncinate fasciculi.

As a secondary analysis, along tract variations in QA between blind and sighted groups were assessed for each reconstructed fasciculus (Colby *et al.*, 2012). A permutation analysis using 10,000 permutations was used to control for family wise error and multiple comparisons.

Results

The uncinate and arcuate fasciculi were reliably reconstructed bilaterally for each subject. In agreement with known anatomy, the uncinate and arcuate fasciculi connected frontal to temporal regions either arching medially around the insula, or posteriorly around the Sylvian fissure, respectively (Kamali *et al.*, 2014; Fernández-Miranda *et al.*, 2015; Hau *et al.*, 2016). Representative example reconstructions from a blind and sighted subject are shown in Figure 1. Prior to adjusting for intracranial volume, the left uncinate was significantly larger than the right in the sighted control group (1060.5 mm3 ± 224.3 SD compared to 1355.0 mm3 ± 480.5 SD respectively; $t(18.41) = -2.08$, $p = 0.05$), while there was no statistically significant difference between the tract volume of the left and right uncinate fasciculi in the blind group (1429.1 mm3 ± 371.3 SD compared to 1557.0 mm3 ± 420.4 SD, respectively; $t(24) = -0.82$, $p = 0.42$). However, no effect of laterality was observed for tract volume within the uncinate fasciculi in either the blind ($t(24)=0.23$, $p = 0.82$) or sighted ($t(18.527)= -1$ $p = 0.32$) groups after adjusting for intracranial volume. With regards to the arcuate fasciculus, prior to adjusting for intracranial volume, the left arcuate was significantly larger than the right in the sighted control group (2596.9 mm3± 821.2 SD compared to 19.71.7 mm3 ± 639.2 SD; $t(26) = 2.25$, $p = 0.03$). However, no statistically significant difference was observed between the left and right arcuate tract volumes in the blind group. (2674.8 mm3 ± 1022.8 SD compared to 2281.1 mm3 ± 752.2 SD, respectively; $t(24) = 1.12$, $p = 0.27$). No effect of laterality with respect to arcuate tract volume was observed after adjusting for intracranial volume in either the blind $t(24) = -028$, $p = 0.78$) or sighted control ($t(26) = 0.50$, $p = 0.62$) groups. Thus, the left and right reconstructions were queried separately for further analysis.

Investigating the variables related to structural integrity revealed that the volume of the left uncinate was larger in the early blind individuals compared to sighted controls (232.9 mm3 ± 370.6 SD compared to −134.6 mm3 ± 221.7 SD respectively; $t(25) = -3.16$, $p = 0.0041$, $p_{Bonferroni} = 0.033$), while the right uncinate volume was not significantly different between groups after correcting for intracranial volume (blind = 197.6 mm3 ± 395.9 SD, control = 4.5 mm3 ± 469.3 SD; $t(25) = -1.15$, $p = 0.26$). Likewise, neither volume of the left arcuate (blind = 142.1 mm3 ± 1023.4 SD, control = 71.29 mm3 ± 819.9 SD; $t(25) = -0.20$, $p = 0.84$) nor right arcuate (blind = 240.0 mm3 ± 752.1 SD, control = −67l.2 mm3 ± 641.1 SD; $t(25) = -1.14$, $p = 0.26$) were significantly different between groups (Figure 2).

Mean QA of the uncinate did not differ significantly between groups for either the left ((blind = 0.18 ± 0.05 SD, control = 0.17 ± 0.07 SD; $t(25) = -0.48$, $p = 0.64$) or right fasciculi (blind = 0.18 ± 0.05 SD, control = 0.17 ± 0.07 SD; $t(25) = -0.74$, $p = 0.47$). Similarly, mean QA of the arcuate also did not differ significantly between groups for either the left ((blind = 0.20 ± 0.06 SD, control = 0.18 ± 0.07 SD; $t(25) = -0.77$, $p = 0.45$) or right fasciculi (blind = 0.21 ± 0.05 SD, control = 0.18 ± 0.06 SD; $t(25) = -1.25$, $p = 0.22$) (Figure 3).

Finally, along tract analysis did not reveal any significant differences in QA between blind and control groups for the uncinate fasciculus bilaterally, or for the left arcuate fasciculus. In

the right arcuate fasciculus, a small area of increased QA was observed approximately half way along the tract (adjusted p = 0.017)(Figure 4).

Discussion

In this study, we compared the structural white matter properties of the arcuate and uncinate fasciculi using HARDI and found an increased volume of the uncinate fasciculus in early blind individuals compared to sighted controls. The exact physiological significance of this increased fiber volume remains indeterminate at this juncture, as it may reflect an increased number of axons, larger axon diameter, or increased axonal myelination within the tract (Ocklenburg *et al.*, 2014). However, all of these possibilities have been associated with more efficient transmission of action potentials (Hodgkin & Rushton, 1946; Hodgkin & Huxley, 1952), which in turn may reflect improved communication between the frontal and temporal lobes (Ocklenburg *et al.*, 2014).

Given the broad functions supported by the uncinate fasciculus, it is difficult to ascertain how an increase in white matter fiber volume is associated with potential behavioral differences in performance in blind individuals. Previous behavioral and neuroimaging studies suggest that early blind individuals demonstrate increased abilities in auditory processing (Arno *et al.*, 2001; Fieger *et al.*, 2006) and verbal/auditory working memory (Amedi *et al.*, 2003; Withagen *et al.*, 2013). These observations of enhanced behavioral performance may be mediated by a combination of both crossmodal changes at the level of occipital cortical areas, as well as changes in the structural properties of key white matter pathways such as the uncinate fasciculus as observed in this study.

In our analyses, we also observed a left lateral asymmetry for both the uncinate and arcuate fasciculi in our sighted control group prior to adjusting for intracranial volume. This left asymmetry has also been reported previously in normally sighted individuals (Kubicki *et al.*, 2002; Fernández-Miranda *et al.*, 2015; Vassal *et al.*, 2016). A leftward-biased laterality has also been previously described in areas connected by the uncinate and arcuate fasciculi, with an increased volume in both Broca's and Wernicke's areas (Parker *et al.*, 2005) and stronger cortical activation in the left language network (Binder *et al.*, 1997). In our sample, this asymmetry was not present in the ocular blind group, and may provide further evidence for structural differences implicating the language system in individuals with early onset blindness.

Lastly, we observed a small area of increased QA in the middle of the right arcuate fasciculus was observed in the blind group. QA is often used to indicate overall white matter structural integrity (Yeh *et al.*, 2010) and may reflect the underlying white matter organization, whereby higher anisotropy is indicative of more cohesively organized tracts (Budde & Annese, 2013).

The results of this study contribute to our growing knowledge regarding the dramatic neuroplastic changes that occur as a result of early and profound blindness. Given the relatively small size of this study, these findings await further confirmation in a larger population sample (Poldrack *et al.*, 2017). Although minimal changes in QA were observed

in our sample, these changes may appear to be more robust in a larger sample. In this study, enrollment of a large sample population remains challenging given our strict criterion of documented profound blindness prior to the age of three, and residual vision no greater than light perception. Future studies with a larger population, perhaps implicating a multi-center study, is warranted to confirm these early findings. Furthermore, future studies should also assess structural-functional relationships in order to uncover the potential association between observed increases in the left uncinate fasciculus volume and various behavioral tasks supported by this white matter pathway.

In conclusion, reported compensatory changes in non-visual modalities present in early blind individuals may not solely be governed by crossmodal changes implicating the occipital lobe. The results of this study indicate that structural changes implicating key white matter pathways supporting non-visual functions, such as the uncinate fasciculus, may also play a key role.

Acknowledgements:

The authors would like to thank all the participants that took part in this study. We would also like to thank Emma Bailin for her help preparing the manuscript and figures for publication. This work was supported by the Research to Prevent Blindness/Lions Clubs International Foundation and National Institutes of Health (R01 EY019924-08) to L.B.M and the Knights Templar Eye Foundation Career Starter Grant and the Deborah Munroe Noonan Memorial Research Fund O'Brien Award to C.M.B.

Abbreviations

HARDI	High angular resolution diffusion imaging
QA	Quantitative anisotropy
DTI	Diffusion tensor imaging
ODF	Orientation distribution function

References

Abhinav K, Yeh F-C, El-Dokla A, Ferrando LM, Chang Y-F, Lacomis D, Friedlander RM, & Fernandez-Miranda JC (2014) Use of diffusion spectrum imaging in preliminary longitudinal evaluation of amyotrophic lateral sclerosis: development of an imaging biomarker. Front. Hum. Neurosci, 8, 270. [PubMed: 24808852]

Amedi A, Raz N, Pianka P, Malach R, & Zohary E (2003) Early "visual" cortex activation correlates with superior verbal memory performance in the blind. Nat. Neurosci, 6, 758–766. [PubMed: 12808458]

Arno P, De Volder AG, Vanlierde A, Wanet-Defalque M-C, Streel E, Robert A, Sanabria-Bohórquez S, & Veraart C (2001) Occipital Activation by Pattern Recognition in the Early Blind Using Auditory Substitution for Vision. NeuroImage, 13, 632–645. [PubMed: 11305892]

Bauer C, Yazzolino L, Hirsch G, Cattaneo Z, Vecchi T, & Merabet LB (2015) Neural correlates associated with superior tactile symmetry perception in the early blind. Cortex J. Devoted Study Nerv. Syst. Behav, 63, 104–117.

Bauer CM, Hirsch GV, Zajac L, Koo B-B, Collignon O, & Merabet LB (2017) Multimodal MR-imaging reveals large-scale structural and functional connectivity changes in profound early blindness. PloS One, 12, e0173064. [PubMed: 28328939]

Berman JI, Lanza MR, Blaskey L, Edgar JC, & Roberts TPL (2013) High angular resolution diffusion imaging probabilistic tractography of the auditory radiation. AJNR Am. J. Neuroradiol, 34, 1573–1578. [PubMed: 23493892]

Binder JR, Frost JA, Hammeke TA, Cox RW, Rao SM, & Prieto T (1997) Human Brain Language Areas Identified by Functional Magnetic Resonance Imaging. J. Neurosci, 17, 353–362. [PubMed: 8987760]

Budde MD & Annese J (2013) Quantification of anisotropy and fiber orientation in human brain histological sections. Front. Integr. Neurosci, 7.

Colby JB, Soderberg L, Lebel C, Dinov ID, Thompson PM, & Sowell ER (2012) Along-tract statistics allow for enhanced tractography analysis. NeuroImage, 59, 3227–3242. [PubMed: 22094644]

Desikan RS, Ségonne F, Fischl B, Quinn BT, Dickerson BC, Blacker D, Buckner RL, Dale AM, Maguire RP, Hyman BT, Albert MS, & Killiany RJ (2006) An automated labeling system for subdividing the human cerebral cortex on MRI scans into gyral based regions of interest. NeuroImage, 31, 968–980. [PubMed: 16530430]

Fernández-Miranda JC, Wang Y, Pathak S, Stefaneau L, Verstynen T, & Yeh F-C (2015) Asymmetry, connectivity, and segmentation of the arcuate fascicle in the human brain. Brain Struct. Funct, 220, 1665–1680. [PubMed: 24633827]

Fieger A, Röder B, Teder-Sälejärvi W, Hillyard SA, & Neville HJ (2006) Auditory spatial tuning in late-onset blindness in humans. J. Cogn. Neurosci, 18, 149–157. [PubMed: 16494677]

Fridriksson J, Guo D, Fillmore P, Holland A, & Rorden C (2013) Damage to the anterior arcuate fasciculus predicts non-fluent speech production in aphasia. Brain J. Neurol, 136, 3451–3460.

Geschwind N (1965) Disconnexion syndromes in animals and man. I. Brain J. Neurol, 88, 237–294.

Greve DN & Fischl B (2009) Accurate and robust brain image alignment using boundary-based registration. NeuroImage, 48, 63–72. [PubMed: 19573611]

Hau J, Sarubbo S, Houde JC, Corsini F, Girard G, Deledalle C, Crivello F, Zago L, Mellet E, Jobard G, Joliot M, Mazoyer B, Tzourio-Mazoyer N, Descoteaux M, & Petit L (2016) Revisiting the human uncinate fasciculus, its subcomponents and asymmetries with stem-based tractography and microdissection validation. Brain Struct. Funct, 1–18.

Hickok G & Poeppel D (2004) Dorsal and ventral streams: a framework for understanding aspects of the functional anatomy of language. Cognition, 92, 67–99. [PubMed: 15037127]

Hodgkin AL & Huxley AF (1952) Propagation of electrical signals along giant nerve fibers. Proc. R. Soc. Lond. B Biol. Sci, 140, 177–183. [PubMed: 13003922]

Hodgkin AL & Rushton W. a. H. (1946) The electrical constants of a crustacean nerve fibre. Proc. R. Soc. Med, 134, 444–479. [PubMed: 20281590]

Kamali A, Sair HI, Radmanesh A, & Hasan KM (2014) Decoding the superior parietal lobule connections of the superior longitudinal fasciculus/arcuate fasciculus in the human brain. Neuroscience, 277C, 577–583.

Karlen SJ, Kahn DM, & Krubitzer L (2006) Early blindness results in abnormal corticocortical and thalamocortical connections. Neuroscience, 142, 843–858. [PubMed: 16934941]

Kubicki M, Westin C-F, Maier SE, Frumin M, Nestor PG, Salisbury DF, Kikinis R, Jolesz FA, McCarley RW, & Shenton ME (2002) Uncinate fasciculus findings in schizophrenia: a magnetic resonance diffusion tensor imaging study. Am. J. Psychiatry, 159, 813–820. [PubMed: 11986136]

Marchina S, Zhu LL, Norton A, Zipse L, Wan CY, & Schlaug G (2011) Impairment of speech production predicted by lesion load of the left arcuate fasciculus. Stroke J. Cereb. Circ, 42, 2251–2256.

Merabet LB & Pascual-Leone A (2010) Neural reorganization following sensory loss: the opportunity of change. Nat. Rev. Neurosci, 11, 44–52. [PubMed: 19935836]

Ocklenburg S, Schlaffke L, Hugdahl K, & Westerhausen R (2014) From structure to function in the lateralized brain: How structural properties of the arcuate and uncinate fasciculus are associated with dichotic listening performance. Neurosci. Lett, 580, 32–36. [PubMed: 25093701]

Olson IR, Heide RJVD, Alm KH, & Vyas G (2015) Development of the uncinate fasciculus: Implications for theory and developmental disorders. Dev. Cogn. Neurosci, 14, 50–61. [PubMed: 26143154]

Papagno C (2011) Naming and the role of the uncinate fasciculus in language function. Curr. Neurol. Neurosci. Rep, 11, 553–559. [PubMed: 21853238]

Parker GJM, Luzzi S, Alexander DC, Wheeler-Kingshott CAM, Ciccarelli O, & Lambon Ralph MA (2005) Lateralization of ventral and dorsal auditory-language pathways in the human brain. NeuroImage, 24, 656–666. [PubMed: 15652301]

Pintzka CWS, Hansen TI, Evensmoen HR, & Håberg AK (2015) Marked effects of intracranial volume correction methods on sex differences in neuroanatomical structures: a HUNT MRI study. Front. Neurosci, 9.

Poldrack RA, Baker CI, Durnez J, Gorgolewski KJ, Matthews PM, Munafò MR, Nichols TE, Poline J-B, Vul E, & Yarkoni T (2017) Scanning the horizon: towards transparent and reproducible neuroimaging research. Nat. Rev. Neurosci, 18, 115–126. [PubMed: 28053326]

Ptito M, Schneider FCG, Paulson OB, & Kupers R (2008) Alterations of the visual pathways in congenital blindness. Exp. Brain Res, 187, 41–49. [PubMed: 18224306]

Ricciardi E, Handjaras G, & Pietrini P (2014) The blind brain: How (lack of) vision shapes the morphological and functional architecture of the human brain. Exp. Biol. Med, 239, 1414–1420.

Sanfilipo MP, Benedict RHB, Zivadinov R, & Bakshi R (2004) Correction for intracranial volume in analysis of whole brain atrophy in multiple sclerosis: the proportion vs. residual method. NeuroImage, 22, 1732–1743. [PubMed: 15275929]

Schaeffer DJ, Krafft CE, Schwarz NF, Chi L, Rodrigue AL, Pierce JE, Allison JD, Yanasak NE, Liu T, Davis CL, & McDowell JE (2014) The relationship between uncinate fasciculus white matter integrity and verbal memory proficiency in children. Neuroreport, 25, 921–925. [PubMed: 24949818]

Seunarine KK & Alexander DC (2014) Multiple Fibers In Diffusion MRI. Elsevier, pp. 105–123.

Tuch DS, Reese TG, Wiegell MR, Makris N, Belliveau JW, & Wedeen VJ (2002) High angular resolution diffusion imaging reveals intravoxel white matter fiber heterogeneity. Magn. Reson. Med. Off. J. Soc. Magn. Reson. Med. Soc. Magn. Reson. Med, 48, 577–582.

Vassal F, Schneider F, Boutet C, Jean B, Sontheimer A, & Lemaire J-J (2016) Combined DTI Tractography and Functional MRI Study of the Language Connectome in Healthy Volunteers: Extensive Mapping of White Matter Fascicles and Cortical Activations. PloS One, 11, e0152614. [PubMed: 27029050]

Von Der Heide RJ, Skipper LM, Klobusicky E, & Olson IR (2013) Dissecting the uncinate fasciculus: disorders, controversies and a hypothesis. Brain J. Neurol, 136, 1692–1707.

Voss P & Zatorre RJ (2012) Organization and Reorganization of Sensory-Deprived Cortex. Curr. Biol, 22, R168–R173. [PubMed: 22401900]

Wilson SM, Galantucci S, Tartaglia MC, Rising K, Patterson DK, Henry ML, Ogar JM, DeLeon J, Miller BL, & Gorno-Tempini ML (2011) Syntactic processing depends on dorsal language tracts. Neuron, 72, 397–403. [PubMed: 22017996]

Withagen A, Kappers AML, Vervloed MPJ, Knoors H, & Verhoeven L (2013) Short term memory and working memory in blind versus sighted children. Res. Dev. Disabil, 34, 2161–2172. [PubMed: 23643769]

Yeh F-C & Tseng W-YI (2013) Sparse Solution of Fiber Orientation Distribution Function by Diffusion Decomposition. PLoS ONE, 8, e75747. [PubMed: 24146772]

Yeh F-C, Wedeen VJ, & Tseng W-YI (2010) Generalized q-sampling imaging. IEEE Trans. Med. Imaging, 29, 1626–1635. [PubMed: 20304721]

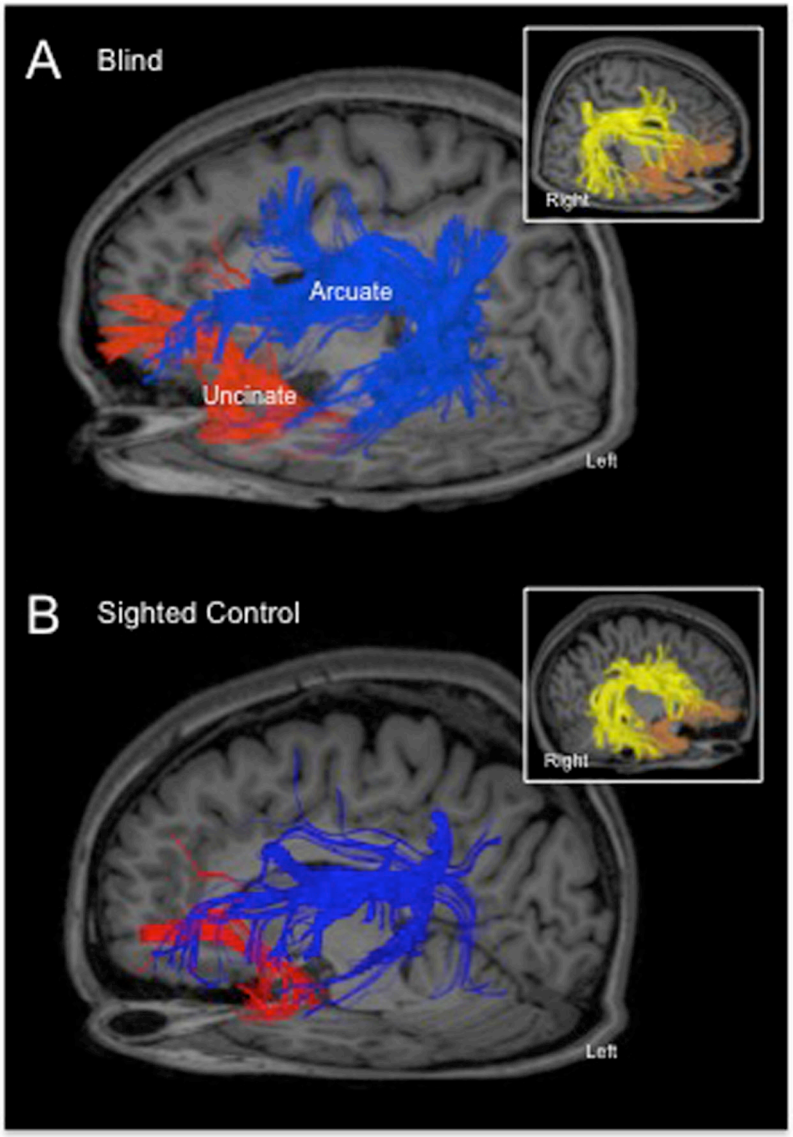

Figure 1.

Example reconstructions of the left (A, B) and right (inset) arcuate and uncinate fasciculi in a representative early blind (A) and sighted control (B) subject. The reconstructions are overlaid on each subject's representative T_1-weighted image. Color coding: red = left uncinate, orange = right uncinate, blue = left arcuate, yellow = right arcuate.

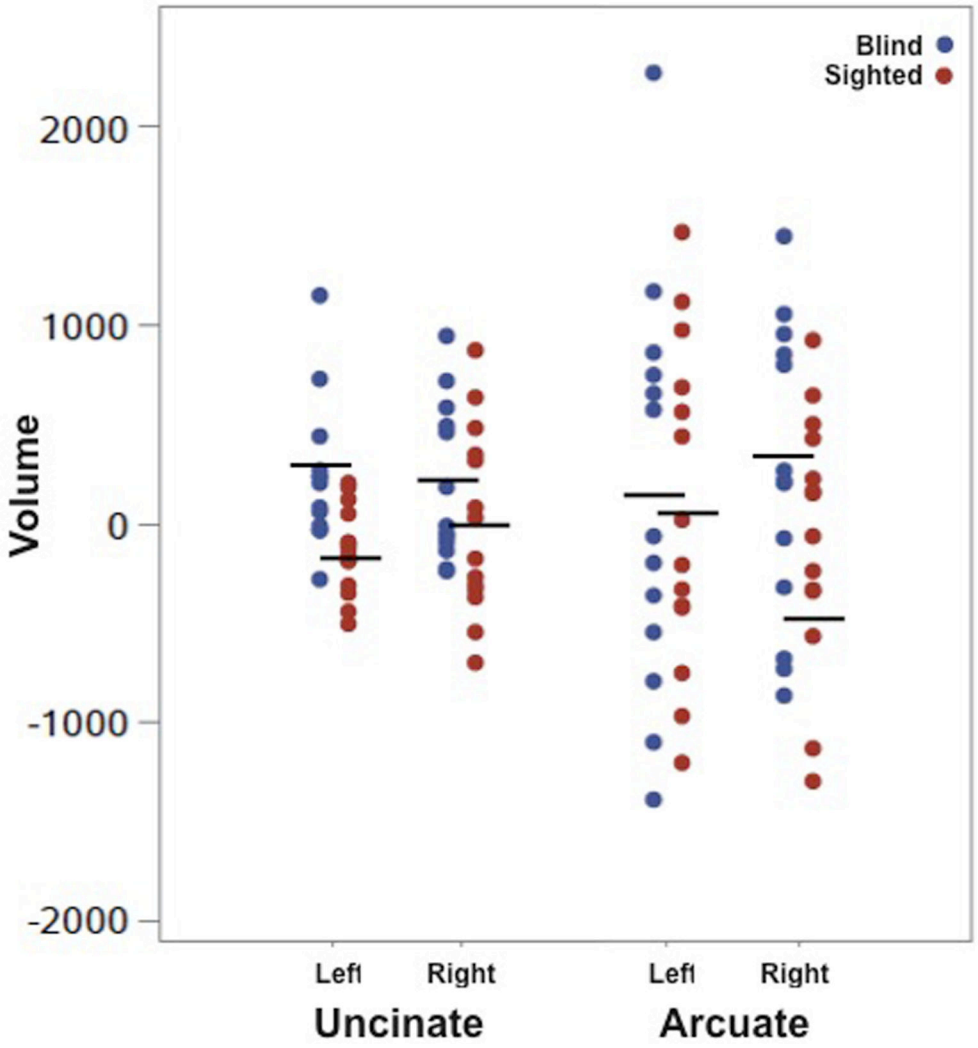

Figure 2.

Left and right volumes of the uncinate and arcuate fasciculi in early blind (blue) and sighted control (red) participants. Significant increases in volume associated with early blindness were observed only for the left uncinate fasciculus, as marked with an asterisk. Tract volume was normalized using residuals for intra-cranial volume for each subject independently and comparisons were made on these residuals, and centered on zero.

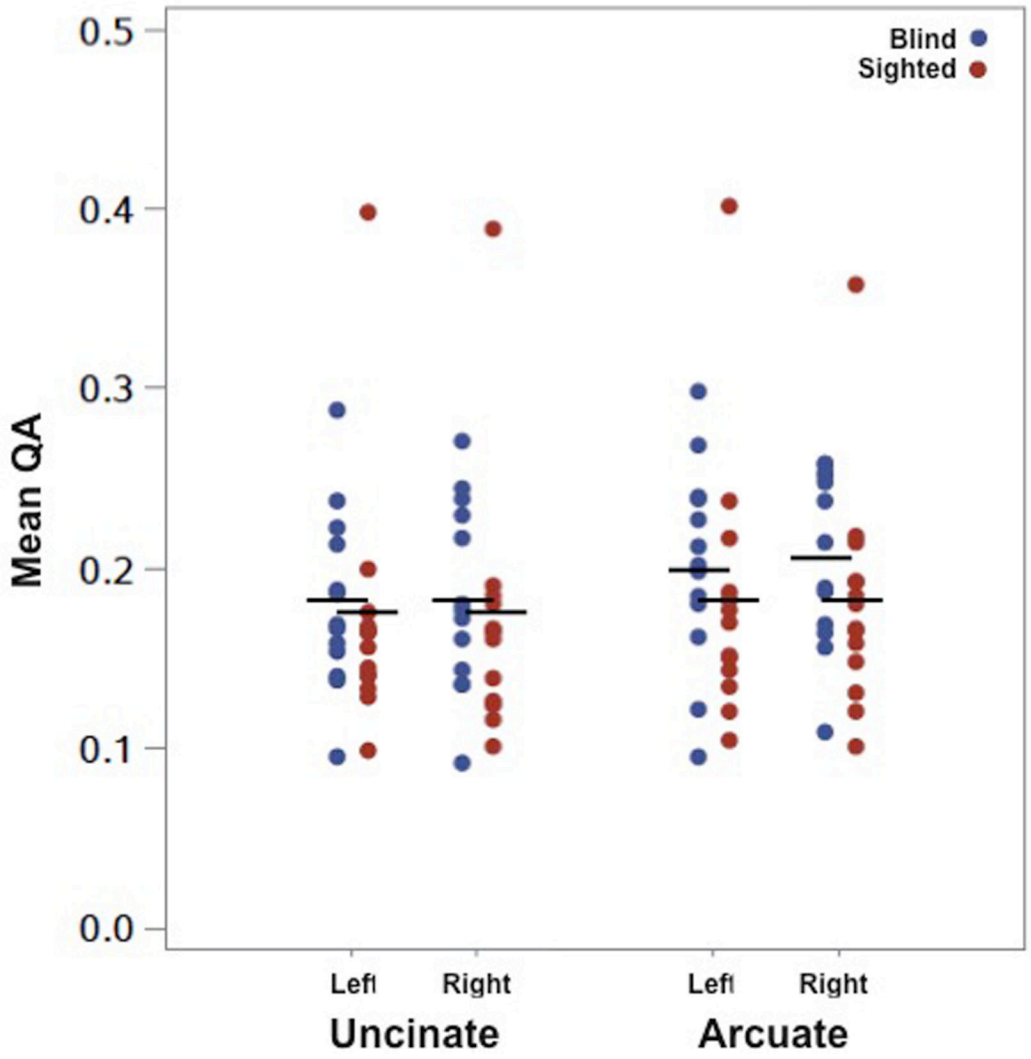

Figure 3.
Left and right mean quantitative anisotropy (QA) of the uncinate and arcuate fasciculi in early blind (blue) and sighted control (red) participants. No significant differences in mean QA were observed for any reconstructed fasciculus.

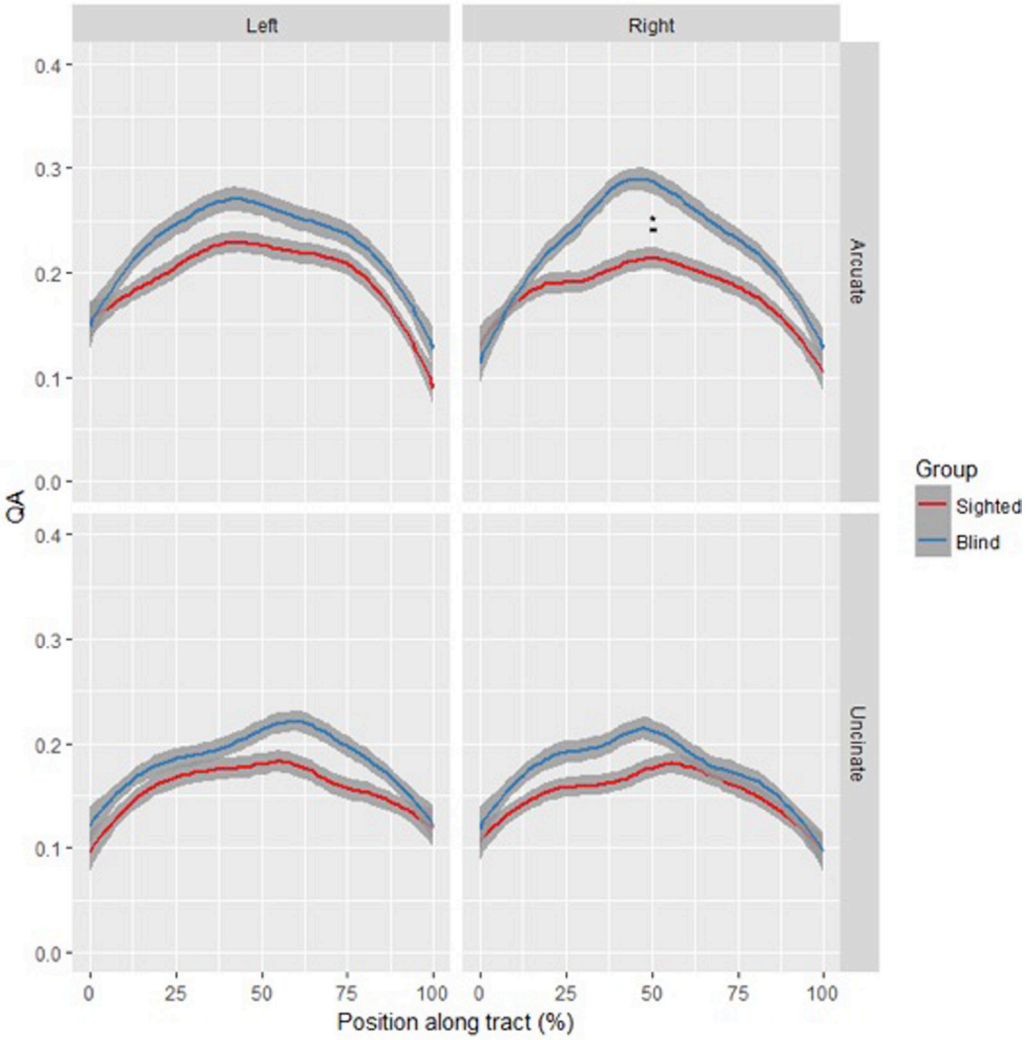

Figure 4.

Along tract analysis of quantitative anisotropy (QA) between early blind (blue) and sighted control (red) participants for the uncinate (bottom) and arcuate (top) fasciculi (left and right shown separately). The mean group data along with the 95% confidence intervals are represented by the dark line and surrounding grey band. A small region of the right arcuate fasciculus (marked by a bar and asterisk and corresponding to approximately half way along the tract position) showed a significantly higher QA in the blind group compared to controls (adjusted $p = 0.017$). No additional significant differences in QA along the tracts were observed.

Table 1

Demographics of blind participants

Subject	Age	Gender	Braille Reader	Onset of Blindness	Visual Function	Diagnosis
1	33	M	yes	birth	LP	Congenital retinitis pigmentosa
2	27	M	yes	birth	NLP	Congenital anophthalmia
3	44	M	yes	birth	NLP	Congenital optic nerve atrophy
4	41	M	yes	birth	NLP	Leber's congenital amaurosis
5	37	M	yes	3 y/o	LP	Juvenile macular degeneration/glaucoma
6	25	F	yes	birth	LP	Leber's congenital amaurosis
7	28	F	yes	3 y/o	NLP	Unknown ocular cause
8	29	F	yes	birth	LP	Retinopathy of prematurity
9	30	F	yes	birth	LP	Retinopathy of prematurity
10	46	F	yes	birth	LP	Ocular infection
11	28	F	yes	birth	LP	Retinopathy of prematurity
12	27	M	yes	birth	LP	Leber's congenital amaurosis
13	42	M	yes	birth	LP	Leber's congenital amaurosis

Abbreviations: LP = light perception, NLP = no light perception, y/o = years old, M = male, F = female.